Series expansions for the 3D transverse Ising model at T=0

1994 J. Phys. A: Math. Gen. 27 5425

(http://iopscience.iop.org/0305-4470/27/16/010)

J. Phys. A: Math. Gen. 27 (1994) 5425–5444. Printed in the UK

Series expansions for the 3D transverse Ising model at $T = 0$

Zheng Weihong†, J Oitmaa‡ and C J Hamer§
School of Physics, The University of New South Wales, Sydney, NSW 2052, Australia

Received 8 June 1994

Abstract. Both weak-coupling and strong-coupling series expansions are calculated for the Ising model in a transverse field at zero temperature in three dimensions. Series are obtained for the ground-state energy, the magnetization, the susceptibility, and the energy gaps, on the simple cubic, the body-centred cubic and the face-centred cubic lattices. The analysis of the critical behaviour is consistent with the behaviour predicted by renormalization group theory for the four-dimensional simple Ising model. There is a remarkable degree of universality between all three lattices.

1. Introduction

The Ising model in a transverse field is a simple lattice spin model which describes a number of real systems, as well as being of theoretical interest. Its Hamiltonian is

$$H = -J \sum_{\langle ij \rangle} S_i^z S_j^z - \Gamma \sum_i S_i^x \tag{1.1}$$

where the S_i^x, S_i^z are quantum spin-$\frac{1}{2}$ operators at each site i, and the sums run over all nearest-neighbour pairs $\langle ij \rangle$ and over all sites i, respectively.

The model has been applied to a wide variety of physical systems including order–disorder ferroelectrics, induced moment ferromagnets, and co-operative Jahn–Teller systems. In most of these applications the operators are, in fact, pseudospins acting on the states of two-level systems, and the transverse field describes transitions between these levels. These applications, and others, have been discussed by Stinchcombe (1972) and Birgeneau (1972).

On the theoretical side, it is known that the transverse Ising model Hamiltonian in d dimensions is the quantum Hamiltonian corresponding to the ordinary Euclidean Ising model in $(d+1)$ dimensions (Pfeuty 1976, Suzuki 1976, Fradkin and Susskind 1978, Green *et al* 1979), and can be obtained as an anisotropic limit of the logarithm of the transfer matrix of the latter model. According to the universality hypothesis, both models should have the same critical behaviour. More specifically, the transverse Ising model at zero temperature is in an ordered phase ($\langle S_i^z \rangle \neq 0$) unless Γ exceeds some critical value Γ_c; and near $\Gamma = \Gamma_c$ the critical behaviour of this model as a function of Γ should be the same as that of the four-dimensional Ising model as a function of temperature T.

Now dimension four is the upper critical dimension for the Ising model, beyond which the critical behaviour is that of mean field theory (for a review, see Brezin *et al* 1976). Precisely at dimension four, the mean-field critical behaviour is modified by confluent

† E-mail address: w.zheng@unsw.edu.au
‡ E-mail address: otja@newt.phys.unsw.edu.au
§ E-mail address: c.hamer@unsw.edu.au

logarithmic corrections. Larkin and Khmel'Nitski (1969), followed by Wegner and Riedel (1973) and Brezin *et al* (1973) applied renormalization group (RG) theory to show that the singular behaviour expected for various thermodynamic quantities near T_c is

$$\text{specific heat:} \qquad C \sim (\ln|t|)^{1/3} \tag{1.2}$$

$$\text{susceptibility:} \qquad \chi \sim |t|^{-1}(\ln|t|)^{1/3} \tag{1.3}$$

$$\text{spontaneous magnetization:} \qquad M \sim |t|^{1/2}(\ln|t|)^{1/3} \quad (t \to 0+) \tag{1.4}$$

$$\text{energy gap:} \qquad m \sim \chi^{-1/2} \sim |t|^{1/2}(\ln|t|)^{-1/6} \tag{1.5}$$

where $t = 1 - T/T_c$ is the reduced temperature variable for the 4D Ising model, or $t = 1 - \Gamma/\Gamma_c$ for the transverse Ising model in 3D. Our principal interest is to try and verify these predictions for the transverse Ising model using series-expansion techniques.

Previous analyses of the 4D Ising model include a high-temperature expansion for the susceptibility on a hypercubic lattice by Fisher and Gaunt (1964), and longer expansions for the susceptibility and fouth-field derivative by Gaunt *et al* (1979). Moore (1970) derived expansions for the spin–spin correlation function, but were unable to distinguish any logarithmic effect. Baker (1977) analysed the fourth-field derivative and the susceptibility, and again saw *no* evidence of logarithmic correction terms, obtaining critical indices such that

$$2\Delta - d\nu - \gamma = -0.302 \pm 0.038 \tag{1.6}$$

in violation of the hyperscaling relation predicted by RG theory

$$2\Delta - d\nu - \gamma = 0\,. \tag{1.7}$$

Gaunt *et al* (1979), in their more extensive study, found, on the contrary, that their results were entirely consistent with the RG predictions.

More recently, Vohwinkel and Weisz (1992) have carried out low-temperature expansions of the magnetization, susceptibilities and second moment. They find that their extrapolated series agree well with Monte Carlo data of Jansen *et al* (1989), and also with solutions of the renormalization group equations in the scaling region. They take these results as support for the conclusion that the lattice ϕ^4 theory in four dimensions, which describes the model in the scaling region, has only a trivial continuum limit.

The transverse Ising model at $T = 0$ in three dimensions has also been the subject of several studies. Pfeuty and Elliott (1971) calculated both weak-coupling and strong-coupling series for the model, and showed in fact that the critical behaviour was like that of the 4D Ising model. Yanase, Takeshige and Suzuki (1976) used high-temperature expansions for the correlation function and susceptibility to extrapolate to the $T = 0$ limit, and reached a similar conclusion. Oitmaa and Plischke (1976) used a similar technique for the fluctuation in the long-range order, but were unable to see any crossover to $d = 4$ critical behaviour at $T = 0$. Oitmaa and Coombs (1981) carried out a high-temperature expansion of the susceptibility for the case of general spin S, and this time did see the expected crossover behaviour.

In this paper we calculate both weak-coupling and strong-coupling series expansions for the spin-$\frac{1}{2}$ transverse Ising model at $T = 0$, involving the ground-state energy per site, the susceptibility, the energy gap, and the magnetization. The lattices considered are the simple cubic (SC), the body-centred cubic (BCC) and face-centred cubic (FCC) lattices. Estimates are given of the critical points, critical indices, confluent logarithmic corrections, and universal amplitude ratios at the critical point.

In section 2 of the paper we briefly summarize the method used to obtain the perturbation series. In section 3 the analysis is carried out, and in section 4 our conclusions are presented.

2. Series expansions

The strong-coupling (SC) form, alternatively called the 'high-temperature' (HT) form, of this Hamiltonian will be taken as

$$H = -\sum_i \sigma_i^z - x \sum_{\langle ij \rangle} \sigma_i^x \sigma_j^x - h \sum_i \sigma_i^x \tag{2.1}$$

where $\langle ij \rangle$ denotes nearest-neighbour pairs of sites on a three-dimensional spatial lattice, the σ_i are Pauli matrices acting on a two-state spin variable at each site, and x, which corresponds to the inverse temperature in the 4D Euclidean formulation, is the SC series-expansion parameter. The magnetic field h is introduced in order to calculate the magnetization and the susceptibility. If x is very large, the model can be described by a weak-coupling (WC) or 'low-temperature' (LT) form

$$H' = -\tfrac{1}{4} \sum_{\langle ij \rangle} \sigma_i^z \sigma_j^z - \lambda \sum_i \sigma_i^x - \tfrac{1}{2} h' \sum_i \sigma_i^z \tag{2.2}$$

where the two Hamiltonians are related by

$$H(x) = H'(\lambda)/\lambda \qquad x = 1/(4\lambda) \qquad h = h'/(2\lambda)\,. \tag{2.3}$$

In each case the Hamiltonian without magnetic field (i.e. with $h = 0$) has the form

$$H = H_0 + tV \tag{2.4}$$

where $t = x$ for the case of strong-coupling expansion, or $t = \lambda$ for the weak-coupling expansion. The term H_0 is taken as the unperturbed Hamiltonian, and the term V then acts as a perturbation, which flips the spin on nearest-neighbour pairs of sites $\langle ij \rangle$ for the strong-coupling expansion, or flips the spin on sites i for the weak-coupling expansion.

We have derived long perturbation expansions in the parameter t, using a linked cluster expansion method due to Nickel (1980). The method has been explained in some detail in He *et al* (1990), where the same model was treated in two space dimensions, and the discussion will not be repeated here. Both weak-coupling and strong-coupling series expansions have been calculated for the ground-state energy per site E_0/N (E_0'/N), the susceptibility

$$\chi = -\frac{1}{N} \frac{\partial^2 E_0}{\partial h^2}\bigg|_{h=0} \qquad \chi' = -\frac{1}{N} \frac{\partial^2 E_0'}{\partial h'^2}\bigg|_{h'=0} \tag{2.5}$$

and the energy gap m (m'), and a weak-coupling expansion has been obtained for the magnetization $M' = -(1/N)\partial E_0'/\partial h'\big|_{h'=0}$. From equations (2.3), the relations between the strong-coupling and weak-coupling observables, respectively, are

$$E_0(x) = E_0'(\lambda)/\lambda \tag{2.6}$$

$$\chi(x) = 4\lambda \chi'(\lambda) \tag{2.7}$$

$$m(x) = m'(\lambda)/\lambda \tag{2.8}$$

with $x = 1/(4\lambda)$.

From the ground-state energy, one can define the 'specific heats'

$$C(x) = -\frac{x^2}{N} \frac{\partial^2 E_0}{\partial x^2} \qquad \text{or} \qquad C'(\lambda) = -\frac{\lambda}{N} \frac{\partial^2 E_0'}{\partial \lambda^2} \tag{2.9}$$

which then obey

$$C(x) = C'(\lambda)\,. \tag{2.10}$$

The calculation of the ground-state energy and its derivatives involves a list of connected clusters up to a certain number of sites (vertices) or bonds (edges), while for the calculation

Table 1. The number of clusters generated for each lattice. Here nv is the number of sites, nb is the number of bonds (edges).

		Ground-State energy		Energy gap	
Lattice	Expansion	Order	No of clusters	Order	No of clusters
SC	SC (HT)	$nb = 14$	4309	$nb = 13$	5652
SC	WC (LT)	$nv = 12$	12280	$nv = 11$	6228
BCC	SC (HT)	$nb = 14$	6170	$nb = 13$	7322
BCC	WC (LT)	$nv = 12$	49021	$nv = 11$	16491
FCC	SC (HT)	$nb = 12$	7176	$nb = 11$	7174
FCC	WC (LT)	$nv = 9$	7215	$nv = 7$	497

of the energy gap, both connected and disconnected clusters, including one or more isolated vertices, are needed. Table 1 gives the number of clusters generated for each lattice. The calculated series are listed in tables 2 and 3. Previously, Pfeuty and Elliott (1971) obtained a weak-coupling series for the magnetization and a strong-coupling series for the energy gap on the SC lattice up to order 3, while strong-coupling series up to order 7 for the susceptibility on all three lattices were obtained by Yanase *et al* (1976). Our results agree with these earlier calculations, and add nine new terms for the magnetization series, ten new terms for the energy gap series, and seven new terms for the susceptibility (five in the case of the FCC lattice). The remaining series are new, as far as we are aware.

3. Series analysis

The analysis of these perturbation series was carried out in stages, as follows.

3.1. Power-law singularities

To begin with, the series were analysed using standard Dlog Padé approximant and confluent differential approximant methods (Guttmann 1989), to estimate the critical points and the 'effective' power-law exponents, ignoring for the moment the expected logarithmic corrections. The best behaved series are those for the strong-coupling energy gap: results from $[N/M]$ Dlog Padé approximants to these series are given in table 4. From this table, we estimate that the critical point lies at $x_c = [0.19406(6),\ 0.14084(8),\ 0.09215(7)]$, respectively, for the [SC, BCC, FCC] lattices. In table 5 the Dlog Padé estimates of the critical parameters obtained from all the various series are listed, where the biased estimates were calculated using the critical point values listed above.

It can be seen from table 5 that the 'effective' exponent values for γ are a little greater than 1, for ν are a little greater than 0.5, for β are around 0.42–0.43, and for α are small and uncertain. These values are quite similar to earlier estimates for the 4D Ising model (Moore 1970, Gaunt *et al* 1979) and the transverse Ising model (Pfeuty and Elliott 1971). They also appear qualitatively consistent, as least, with the RG predictions (1.2)–(1.5).

Now there are certain combinations of the observables whose leading singularities should be purely power-behaved, according to (1.2)–(1.5). For instance, one expects $M/C \sim |t|^{1/2}$, $\chi/M \sim |t|^{-3/2}$, $\chi/C \sim |t|^{-1}$, $m^2C \sim |t|$, and $m^2\chi \sim$ constant. To analyse the series for these combinations, we firstly eliminate the effect of any antiferromagnetic singularity by performing an Euler transformation

$$y = 2x/(1 + x/x_c^*) \tag{3.1}$$

Table 2. Strong-coupling (high-temperature) series in x for the ground-state energy per site E_0/N, the susceptibility χ, and the energy gap m of the transverse Ising model. Coefficients of x^n are listed.

n	E_0/N	χ	m
SC lattice			
0	−1	1	2
1	0	6	−6
2	$-7.500\,000\,000\,000\times10^{-1}$	$3.225\,000\,000\,000\times10^{1}$	$-6.000\,000\,000\,000$
3	$0.000\,000\,000\,000$	$1.725\,000\,000\,000\times10^{2}$	$-1.500\,000\,000\,000\times10^{1}$
4	$-1.359\,375\,000\,000$	$9.080\,468\,750\,000\times10^{2}$	$-4.650\,000\,000\,000\times10^{1}$
5	$0.000\,000\,000\,000$	$4.775\,895\,833\,333\times10^{3}$	$-1.725\,000\,000\,000\times10^{2}$
6	$-9.433\,593\,750\,000$	$2.496\,107\,682\,292\times10^{4}$	$-6.316\,171\,875\,000\times10^{2}$
7	$0.000\,000\,000\,000$	$1.304\,100\,138\,889\times10^{5}$	$-2.659\,189\,453\,125\times10^{3}$
8	$-9.680\,401\,611\,328\times10^{1}$	$6.791\,495\,855\,711\times10^{5}$	$-1.060\,257\,824\,707\times10^{4}$
9	$0.000\,000\,000\,000$	$3.536\,163\,533\,925\times10^{6}$	$-4.735\,682\,995\,605\times10^{4}$
10	$-1.241\,021\,419\,525\times10^{3}$	$1.837\,669\,188\,197\times10^{7}$	$-1.983\,770\,115\,700\times10^{5}$
11	$0.000\,000\,000\,000$	$9.548\,768\,040\,118\times10^{7}$	$-9.167\,337\,492\,285\times10^{5}$
12	$-1.828\,322\,336\,101\times10^{4}$	$4.955\,398\,251\,608\times10^{8}$	$-3.967\,955\,605\,458\times10^{6}$
13	$0.000\,000\,000\,000$	$2.571\,415\,145\,418\times10^{9}$	$-1.874\,254\,024\,879\times10^{7}$
14	$-2.959\,553\,663\,348\times10^{5}$	$1.333\,149\,282\,698\times10^{10}$	
BCC lattice			
0	−1	1	2
1	0	8	−8
2	$-1.000\,000\,000\,000$	$5.900\,000\,000\,000\times10^{1}$	$-1.200\,000\,000\,000\times10^{1}$
3	$0.000\,000\,000\,000$	$4.340\,000\,000\,000\times10^{2}$	$-4.200\,000\,000\,000\times10^{1}$
4	$-4.562\,500\,000\,000$	$3.143\,145\,833\,333\times10^{3}$	$-1.740\,000\,000\,000\times10^{2}$
5	$0.000\,000\,000\,000$	$2.274\,983\,333\,333\times10^{4}$	$-8.872\,500\,000\,000\times10^{2}$
6	$-5.804\,687\,500\,000\times10^{1}$	$1.636\,964\,299\,769\times10^{5}$	$-4.505\,250\,000\,000\times10^{3}$
7	$0.000\,000\,000\,000$	$1.177\,594\,879\,823\times10^{6}$	$-2.595\,150\,000\,000\times10^{4}$
8	$-1.133\,810\,546\,875\times10^{3}$	$8.445\,830\,945\,366\times10^{6}$	$-1.435\,225\,275\,879\times10^{5}$
9	$0.000\,000\,000\,000$	$6.056\,641\,148\,835\times10^{7}$	$-8.772\,396\,340\,942\times10^{5}$
10	$-2.768\,589\,859\,772\times10^{4}$	$4.335\,455\,001\,221\times10^{8}$	$-5.096\,307\,178\,719\times10^{6}$
11	$0.000\,000\,000\,000$	$3.103\,141\,112\,826\times10^{9}$	$-3.224\,563\,470\,224\times10^{7}$
12	$-7.759\,160\,598\,470\times10^{5}$	$2.218\,441\,771\,801\times10^{10}$	$-1.934\,986\,229\,311\times10^{8}$
13	$0.000\,000\,000\,000$	$1.585\,878\,065\,228\times10^{11}$	$-1.252\,095\,780\,670\times10^{9}$
14	$-2.388\,247\,818\,341\times10^{7}$	$1.132\,723\,493\,755\times10^{12}$	
FCC lattice			
0	−1	1	2
1	0	12	−12
2	$-1.500\,000\,000\,000$	$1.365\,000\,000\,000\times10^{2}$	$-3.000\,000\,000\,000\times10^{1}$
3	$-3.000\,000\,000\,000$	$1.527\,000\,000\,000\times10^{3}$	$-1.470\,000\,000\,000\times10^{2}$
4	$-1.228\,125\,000\,000\times10^{1}$	$1.694\,290\,625\,000\times10^{4}$	$-9.825\,000\,000\,000\times10^{2}$
5	$-6.187\,500\,000\,000\times10^{1}$	$1.870\,950\,833\,333\times10^{5}$	$-7.336\,125\,000\,000\times10^{3}$
6	$-3.638\,203\,125\,000\times10^{2}$	$2.059\,663\,006\,076\times10^{6}$	$-5.922\,728\,906\,250\times10^{4}$
7	$-2.367\,703\,125\,000\times10^{3}$	$2.262\,540\,374\,913\times10^{7}$	$-5.016\,284\,003\,906\times10^{5}$
8	$-1.657\,379\,077\,148\times10^{4}$	$2.481\,482\,155\,913\times10^{8}$	$-4.401\,691\,375\,122\times10^{6}$
9	$-1.225\,060\,279\,541\times10^{5}$	$2.718\,335\,268\,007\times10^{9}$	$-3.965\,104\,240\,860\times10^{7}$
10	$-9.447\,149\,492\,455\times10^{5}$	$2.974\,977\,513\,949\times10^{10}$	$-3.646\,206\,044\,064\times10^{8}$
11	$-7.536\,782\,435\,456\times10^{6}$	$3.253\,379\,986\,588\times10^{11}$	$-3.408\,623\,105\,456\times10^{9}$
12	$-6.182\,305\,303\,681\times10^{7}$	$3.555\,589\,413\,812\times10^{12}$	

where x_c^* is an estimate of the exact critical point x_c. Then Dlog Padé approximants and confluent differential approximants to the transformed series were calculated. The results obtained are shown in table 6 (where the preferred critical points used in the

Table 3. Weak-coupling (low-temperature) series in λ^2 for the ground-state energy per site E_0'/N, the magnetization M', the susceptibility χ', and the energy gap m of the transverse Ising model. Coefficients of $(\lambda^2)^n$ are listed.

n	E_0'/N	M'	χ'	m'
SC lattice				
0	$-\frac{3}{4}$	$\frac{1}{2}$	0	3
1	$-\frac{1}{3}$	$-\frac{1}{9}$	$\frac{2}{27}$	$-\frac{4}{3}$
2	$-7.407\,407\,407\,407\times10^{-3}$	$-2.518\,518\,518\,519\times10^{-2}$	$5.965\,432\,098\,765\times10^{-2}$	$2.370\,370\,370\,370\times10^{-1}$
3	$-4.703\,115\,814\,227\times10^{-4}$	$-7.334\,621\,091\,235\times10^{-3}$	$3.714\,552\,864\,062\times10^{-2}$	$-4.193\,768\,371\,546\times10^{-1}$
4	$-1.911\,356\,220\,586\times10^{-4}$	$-3.133\,155\,006\,365\times10^{-3}$	$2.440\,762\,229\,285\times10^{-2}$	$4.872\,528\,226\,916\times10^{-1}$
5	$-2.164\,811\,980\,306\times10^{-5}$	$-1.235\,233\,224\,717\times10^{-3}$	$1.472\,173\,854\,186\times10^{-2}$	$-6.979\,931\,014\,337\times10^{-1}$
6	$-1.796\,353\,660\,384\times10^{-5}$	$-6.177\,842\,806\,839\times10^{-4}$	$9.346\,087\,036\,334\times10^{-3}$	$1.000\,570\,272\,574$
7	$-2.946\,525\,630\,590\times10^{-6}$	$-2.790\,562\,317\,414\times10^{-4}$	$5.658\,413\,119\,090\times10^{-3}$	$-1.510\,053\,596\,210$
8	$-2.296\,328\,263\,288\times10^{-6}$	$-1.452\,183\,554\,366\times10^{-4}$	$3.516\,623\,255\,080\times10^{-3}$	$2.343\,670\,970\,861$
9	$-4.693\,484\,241\,776\times10^{-7}$	$-7.023\,368\,199\,928\times10^{-5}$	$2.124\,781\,376\,080\times10^{-3}$	$-3.731\,688\,168\,207$
10	$-3.887\,742\,149\,811\times10^{-7}$	$-3.773\,175\,616\,517\times10^{-5}$	$1.308\,667\,686\,017\times10^{-3}$	$6.054\,197\,893\,638$
11	$-9.343\,649\,339\,950\times10^{-8}$	$-1.907\,194\,514\,459\times10^{-5}$	$7.906\,721\,101\,787\times10^{-4}$	
12	$-7.293\,583\,970\,008\times10^{-8}$	$-1.039\,438\,213\,977\times10^{-5}$	$4.836\,289\,875\,998\times10^{-4}$	
BCC lattice				
0	-1	$\frac{1}{2}$	0	4
1	$-\frac{1}{4}$	$-\frac{1}{16}$	$\frac{1}{32}$	$-\frac{5}{6}$
2	$-2.232\,142\,857\,143\times10^{-3}$	$-6.776\,147\,959\,184\times10^{-3}$	$1.224\,262\,026\,239\times10^{-2}$	$3.687\,169\,312\,169\times10^{-2}$
3	$-5.580\,357\,142\,857\times10^{-5}$	$-9.992\,825\,255\,102\times10^{-4}$	$3.860\,804\,254\,738\times10^{-3}$	$-5.221\,722\,691\,134\times10^{-2}$
4	$-1.957\,231\,424\,507\times10^{-5}$	$-2.322\,041\,501\,665\times10^{-4}$	$1.335\,770\,380\,000\times10^{-3}$	$2.375\,114\,717\,773\times10^{-2}$
5	$-1.207\,665\,353\,680\times10^{-6}$	$-4.886\,340\,516\,567\times10^{-5}$	$4.262\,910\,657\,885\times10^{-4}$	$-1.530\,836\,939\,034\times10^{-2}$
6	$-4.549\,481\,484\,405\times10^{-7}$	$-1.262\,825\,900\,862\times10^{-5}$	$1.412\,688\,250\,449\times10^{-4}$	$9.459\,937\,604\,643\times10^{-3}$
7	$-4.024\,063\,875\,282\times10^{-8}$	$-3.019\,483\,214\,887\times10^{-6}$	$4.499\,583\,283\,742\times10^{-5}$	$-6.300\,603\,374\,835\times10^{-3}$
8	$-1.645\,418\,348\,431\times10^{-8}$	$-8.215\,758\,585\,917\times10^{-7}$	$1.465\,460\,360\,330\times10^{-5}$	$4.263\,687\,933\,437\times10^{-3}$
9	$-1.943\,867\,680\,373\times10^{-9}$	$-2.112\,953\,648\,144\times10^{-7}$	$4.669\,547\,549\,564\times10^{-6}$	$-2.968\,204\,985\,957\times10^{-3}$
10	$-7.518\,643\,482\,234\times10^{-10}$	$-5.908\,769\,768\,623\times10^{-8}$	$1.507\,440\,176\,516\times10^{-6}$	$2.099\,263\,974\,982\times10^{-3}$
11	$-1.089\,495\,959\,150\times10^{-10}$	$-1.588\,701\,042\,712\times10^{-8}$	$4.802\,569\,173\,811\times10^{-7}$	
12	$-3.969\,533\,809\,196\times10^{-11}$	$-4.521\,500\,817\,766\times10^{-9}$	$1.542\,268\,523\,379\times10^{-7}$	
FCC lattice				
0	$-\frac{3}{2}$	$\frac{1}{2}$	0	6
1	$-\frac{1}{6}$	$-\frac{1}{36}$	$\frac{1}{108}$	$-\frac{7}{15}$
2	$-4.208\,754\,208\,754\times10^{-4}$	$-1.128\,711\,355\,984\times10^{-3}$	$1.392\,483\,141\,794\times10^{-3}$	$-1.269\,360\,269\,360\times10^{-2}$
3	$-1.376\,347\,651\,600\times10^{-5}$	$-8.321\,204\,742\,688\times10^{-5}$	$2.021\,212\,801\,814\times10^{-4}$	$-8.603\,484\,011\,312\times10^{-4}$
4	$-6.674\,358\,915\,275\times10^{-7}$	$-7.355\,853\,703\,436\times10^{-6}$	$2.865\,270\,148\,995\times10^{-5}$	$-7.091\,996\,447\,689\times10^{-5}$
5	$-4.181\,512\,501\,399\times10^{-8}$	$-7.177\,108\,434\,326\times10^{-7}$	$4.013\,135\,029\,368\times10^{-6}$	$-6.983\,003\,710\,967\times10^{-6}$
6	$-3.079\,228\,652\,626\times10^{-9}$	$-7.456\,917\,782\,882\times10^{-8}$	$5.584\,520\,083\,258\times10^{-7}$	$-4.427\,236\,297\,102\times10^{-7}$
7	$-2.407\,422\,075\,250\times10^{-10}$	$-8.043\,737\,090\,472\times10^{-9}$	$7.721\,536\,061\,075\times10^{-8}$	
8	$-2.101\,301\,991\,067\times10^{-11}$	$-8.964\,144\,028\,677\times10^{-10}$	$1.064\,268\,397\,556\times10^{-8}$	
9	$-1.942\,081\,382\,111\times10^{-12}$	$-1.023\,260\,133\,901\times10^{-10}$	$1.463\,661\,247\,996\times10^{-9}$	

biased estimates are obtained from the later analysis). It can be seen that the critical exponent estimates (residues) for the weak-coupling series are reasonably consistent with the expected values, to within an accuracy of 5% or so. The series for $m^2\chi$ shows no evidence of singular behaviour. The strong-coupling series are not so well behaved, however.

A further test of the power-law exponents can be made by dividing out the expected logarithmic corrections. Assuming the critical point is known, each series can be multiplied

Table 4. Dlog Padé approximants to the strong-coupling (HT) energy gap series. An asterisk denotes a defective approximant.

N	$[N/N-1]$ Pole (residue)	$[N/N]$ Pole (residue)	$[N/N+1]$ Pole (residue)
SC lattice			
2	0.196 152(0.577 350)	0.196 081(0.576 715)	0.194 825(0.563 611)
3	0.194 192(0.552 952)	0.194 625(0.560 522)	0.196 827(0.522 489)*
4	0.194 480(0.557 851)	0.194 049(0.545 899)	0.194 107(0.548 016)
5	0.194 101(0.547 781)	0.194 078(0.546 916)	0.194 063(0.546 329)
6	0.194 061(0.546 230)	0.194 094(0.547 430)*	
BCC lattice			
2	0.141 694(0.564 296)	0.141 588(0.563 011)	0.141 345(0.559 076)
3	0.141 825(0.564 778)*	0.140 036(0.504 448)*	0.140 932(0.548 712)
4	0.141 146(0.555 995)	0.140 869(0.546 289)	0.140 840(0.544 968)
5	0.140 848(0.545 349)	0.140 905(0.547 443)*	0.140 777(0.541 366)*
6	0.140 803(0.543 097)	0.140 762(0.540 309)*	
FCC lattice			
2	0.092 763(0.564 986)	0.092 492(0.558 737)	0.092 551(0.560 040)*
3	0.092 129(0.543 978)	0.092 190(0.547 238)	0.092 164(0.545 699)
4	0.092 173(0.546 258)	0.092 115(0.541 807)*	0.091 883(0.499 527)*
5	0.091 979(0.521 730)*	0.092 082(0.538 216)*	

Table 5. *Estimates of singularity parameters for the second-order phase transitions, obtained by* Dlog Padé approximants to the series listed in table 2 and 3. Both biased (b) and unbiased (ub) estimates are listed.

Series	WC (LT)			SC (HT)		
	Pole	Residue		Pole	Residue	
		ub	b		ub	b
SC lattice: the critical point biased at $x_c = 0.194\,06(6)$, $\lambda_c^2 = 1.659\,6(10)$						
C	$\lambda_c^2 = 1.72(5)$	$\alpha = 0.14(3)$	0.07(4)	$x_c^2 = 0.040(3)$	$\alpha = 0.3(2)$	0.2(1)
M	$\lambda_c^2 = 1.662(5)$	$\beta = 0.43(2)$	0.425(7)			
χ	$\lambda_c^2 = 1.67(1)$	$\gamma = 1.17(6)$	1.11(5)	$x_c = 0.194\,0(4)$	$\gamma = 1.08(2)$	1.086(8)
m	$\lambda_c^2 = 1.66(4)$	$\nu = 0.5(1)$	0.555(10)	$x_c = 0.194\,06(6)$	$\nu = 0.547(2)$	0.546(2)
BCC lattice: the critical point biased at $x_c = 0.140\,84(8)$, $\lambda_c^2 = 3.151(4)$						
C	$\lambda_c^2 = 3.23(8)$	$\alpha = 0.12(4)$	0.07(2)	$x_c^2 = 0.021(1)$	$\alpha = 0.3(2)$	0.2(1)
M	$\lambda_c^2 = 3.151(4)$	$\beta = 0.426(7)$	0.428(6)			
χ	$\lambda_c^2 = 3.16(1)$	$\gamma = 1.14(6)$	1.09(5)	$x_c = 0.140\,8(1)$	$\gamma = 1.08(1)$	1.084(10)
m	$\lambda_c^2 = 3.1(3)$	$\nu = 0.5(1)$	0.543(6)	$x_c = 0.140\,84(8)$	$\nu = 0.542(6)$	0.545(4)
FCC lattice: the critical point biased at $x_c = 0.092\,15(7)$, $\lambda_c^2 = 7.36(1)$						
C	$\lambda_c^2 = 7.8(10)$	$\alpha = 0.13(3)$	0.08(3)	$x_c = 0.093\,7(6)$	$\alpha = 0.3(2)$	0.23(15)
M	$\lambda_c^2 = 7.36(4)$	$\beta = 0.42(2)$	0.428(7)			
χ	$\lambda_c^2 = 7.41(4)$	$\gamma = 1.16(3)$	1.12(5)	$x_c = 0.092\,1(1)$	$\gamma = 1.08(2)$	1.084(10)
m	$\lambda_c^2 = 7.38(2)$	$\nu = 0.56(1)$	0.555(8)	$x_c = 0.092\,15(7)$	$\nu = 0.545(10)$	0.545(5)

Specific heat: $C \sim (x_c - x)^{-\alpha}$.
Magnetization: $M \sim (x_c - x)^{\beta}$.
Susceptibility: $\chi \sim (x_c - x)^{-\gamma}$.
Energy gap: $m \sim (x_c - x)^{\nu}$.

by another series which cancels out the logarithmic correction terms listed in (1.2)–(1.5), and the resultant series can be analysed for power-law singularities using Dlog Padé

Table 6. Estimates of singularity parameters obtained by Dlog Padé approximants and confluent different differential approximants to selected combinations of the series listed in tables 2 and 3. Both biased (b) and unbiased (ub) estimates are listed.

Series	WC (LT)			SC (HT)		
	Pole	Residue		Pole	Residue	
		ub	b		ub	b
SC lattice: the critical point biased at $x_c = 0.19386(2)$, $\lambda_c^2 = 1.6630(3)$						
M/C	$\lambda_c^2 = 1.665(3)$	0.54(2)	0.52(2)			
χ/M	$\lambda_c^2 = 1.664(5)$	−1.57(5)	−1.55(4)			
χ/C	$\lambda_c^2 = 1.664(10)$	−1.04(5)	−1.03(4)	$x_c = 0.193(4)$	−0.7(3)[a]	−0.9(1)
m^2C	$\lambda_c^2 = 1.66(4)$	1.0(1)	1.02(3)	$x_c = 0.193(3)$	0.7(4)[a]	1.0(1)
$m^2\chi$	no pole found			$x_c = 0.20(1)$	0.01(1)	0.005(5)
BCC lattice: the critical point biased at $x_c = 0.14071(8)$, $\lambda_c^2 = 3.157(3)$						
M/C	$\lambda_c^2 = 3.161(5)$	0.53(3)	0.52(2)			
χ/M	$\lambda_c^2 = 3.159(5)$	−1.56(4)	−1.54(3)			
χ/C	$\lambda_c^2 = 3.161(4)$	−1.04(3)	−1.02(2)	$x_c = 0.14(1)$	−0.7(2)[a]	−0.9(1)
m^2C	$\lambda_c^2 = 3.16(2)$	1.00(5)	1.002(5)	$x_c = 0.14(1)$	0.8(3)[a]	1.0(1)
$m^2\chi$	no pole found			$x_c = 0.147(4)$	0.01(1)	0.003(3)
FCC lattice: the critical point biased at $x_c = 0.09206(2)$, $\lambda_c^2 = 7.375(3)$						
M/C	$\lambda_c^2 = 7.39(2)$	0.54(3)	0.54(2)			
χ/M	$\lambda_c^2 = 7.38(1)$	−1.56(4)	−1.53(4)			
χ/C	$\lambda_c^2 = 7.37(2)$	−1.02(2)	−1.02(1)	$x_c = 0.0916(10)$	−0.7(2)[a]	−0.8(2)
m^2C	$\lambda_c^2 = 7.38(5)$	1.02(4)	1.02(2)	$x_c = 0.0915(10)$	0.7(2)[a]	1.0(1)
$m^2\chi$	no pole found			$x_c = 0.095(4)$	0.01(1)	0.004(4)

[a] All estimates defective.

Table 7. Biased estimates of power-law exponents for the series listed in tables 2 and 3, with the expected logarithmic corrections cancelled out using multiplier functions $t_1 = [-\ln(1 - x/x_c)/(x/x_c)]^{-1/3}$, $t_2 = [-\ln(1 - x/x_c)/(x/x_c)]^{1/6}$.

Series	WC (LT)		SC (HT)	
	Residue	RG prediction	Residue	RG prediction
SC lattice: the critical point biased at $x_c = 0.19386(2)$, $\lambda_c^2 = 1.6630(3)$				
t_1C	no pole found	no pole	−0.1(1)	no pole
t_1M	0.52(2)	0.5		
$t_1\chi$	−1.03(2)	−1	−0.99(1)	−1
t_2m	0.51(1)	0.5	0.496(10)	0.5
BCC lattice: the critical point biased at $x_c = 0.14071(8)$, $\lambda_c^2 = 3.157(3)$				
t_1C	no pole found	no pole	−0.15(10)	no pole
t_1M	0.52(2)	0.5		
$t_1\chi$	−1.01(2)	−1	−0.99(2)	−1
t_2m	0.50(1)	0.5	0.50(1)	0.5
FCC lattice: the critical point biased at $x_c = 0.09206(2)$, $\lambda_c^2 = 7.375(3)$				
t_1C	no pole found	no pole	−0.15(10)	no pole
t_1M	0.53(2)	0.5		
$t_1\chi$	−1.01(1)	−1	−0.98(2)	−1
t_2m	0.50(1)	0.5	0.496(10)	0.5

approximants as usual. The results are shown in table 7. Again, the power-law exponents are very close to the expected values, within errors of 2–5%.

Table 8. Biased estimates of the logarithmic indices p for various series. Power-law singularities have been multiplied out where necessary using functions $t_1 = (1 - x/x_c)^{-1/2}$, $t_2 = (1 - x/x_c)$

Series	WC (LT) Residue	WC (LT) RG prediction	SC (HT) Residue	SC (HT) RG prediction
SC lattice: the critical point biased at $x_c = 0.193\,86(2)$, $\lambda_c^2 = 1.663\,0(3)$				
C	0.36(4)	$\frac{1}{3}$	0.8(2)	$\frac{1}{3}$
χM^2	0.99(1)	1		
M/m	0.47(8)	$\frac{1}{3}$		
χm^2	no pole found	no pole	−0.02(2)	no pole
$t_1 M$	0.29(4)	$\frac{1}{3}$		
$t_2 \chi$	0.39(5)	$\frac{1}{3}$	0.29(5)	$\frac{1}{3}$
$t_1 m$	−0.15(5)	$-\frac{1}{6}$	−0.143(5)	$-\frac{1}{6}$
BCC lattice: the critical point biased at $x_c = 0.140\,71(8)$, $\lambda_c^2 = 3.157(3)$				
C	0.33(4)	$\frac{1}{3}$	0.8(1)	$\frac{1}{3}$
χM^2	0.9(1)	1		
M/m	0.4(1)	$\frac{1}{2}$		
χm^2	no pole found	no pole	−0.02(2)	no pole
$t_1 M$	0.27(3)	$\frac{1}{3}$		
$t_2 \chi$	0.34(3)	$\frac{1}{3}$	0.30(4)	$\frac{1}{3}$
$t_1 m$	−0.13(3)	$-\frac{1}{6}$	−0.14(2)	$-\frac{1}{6}$
FCC lattice: the critical point biased at $x_c = 0.092\,06(2)$, $\lambda_c^2 = 7.375(3)$				
C	0.33(4)	$\frac{1}{3}$	1.01(1)	$\frac{1}{3}$
χM^2	0.85(15)	1		
M/m	0.4(1)	$\frac{1}{2}$		
χm^2	no pole found	no pole	−0.02(2)	no pole
$t_1 M$	0.27(4)	$\frac{1}{3}$		
$t_2 \chi$	0.32(5)	$\frac{1}{3}$	0.26(8)	$\frac{1}{3}$
$t_1 m$	−0.17(3)	$-\frac{1}{6}$	−0.15(2)	$-\frac{1}{6}$

3.2. *Confluent logarithmic singularities*

It is well known that it is virtually impossible to distinguish a logarithmic singularity from a weak power-law singularity by numerical means. The best we can do is to apply various consistency tests, assuming from the start that the power-law exponents are those given by the RG predictions (1.2)–(1.5),

To begin with, there are certain combinations of observables whose leading singularities should be purely logarithmic. For instance, the RG predicts $C \sim |\ln|t||^{1/2}$, $\chi M^2 \sim \ln|t|$, and $M/m \sim |\ln|t||^{1/2}$. Now if a function $f(x)$ has a logarithmic singularity of the form

$$f(x) \sim A(x)\left|\ln\left|1 - \frac{x}{x_c}\right|\right|^p \tag{3.2}$$

where $A(x)$ is analytic, then for x near x_c we have

$$\frac{\ln(1 - x/x_c)}{(x/x_c)}\frac{1}{f}\frac{\mathrm{d}f}{\mathrm{d}x} \sim \frac{p}{x - x_c}. \tag{3.3}$$

Thus, given a previous estimate of the critical point x_c, we can obtain a biased estimate of the index p by forming a Padé approximants to the series for the left-hand side of equation (3.3). A similar method can be applied to the original observables M, χ and m, once the expected power-law singularities have been 'multiplied out'. The results of such an analysis are shown in table 9. The estimates of the logarithmic indices p are generally in quite reasonable agreement with the predicted values, at a level of accuracy 10–20%.

Another method of analysis was proposed by Guttmann (1978, 1989), and employed previously by Gaunt *et al* (1978). We shall apply it to the weak-coupling susceptibility, which is the best-behaved series for this purpose. Assume the series behaves as

$$\chi(x) = A(x)(1 - x/x_c)^{-q}|\ln(1 - x/x_c)|^p \tag{3.4}$$

where $A(x)$ is analytic near $x = x_c$, and the exponent q is known, $q = 1$. Again, the analysis begins by eliminating the effect of any antiferromagnetic singularity by performing an Euler transformation as in (3.1). Writing the transformed series as

$$\chi(y) = \sum_n a_n y^n \tag{3.5}$$

we next calculate the ratios $r_n = a_n/a_{n-1}$. Then defining another function $f(y)$ by

$$f(y) = (1 - y)^{-q^*}|\ln(1 - y)/y|^{p^*} = \sum_n b_n y^n \tag{3.6}$$

with $q^* = 1$, we calculate the ratios $r_n^* = b_n/b_{n-1}$. The basic aim is now to compare the behaviour of the ratio r_n^* for the mimic function $f(x)$ with the behaviour of the r_n for a range of values of the parameter p^*. The analysis is based upon the following two observations. Firstly, as $n \to \infty$ the sequence $R_n = r_n/r_n^*$ should approach x_c^{-1} with zero slope when $p^* = p$. To allow for higher-order correction terms, the following extrapolants are calculated:

$$R_n = R_\infty + \sum_{i=1}^{N} c_i/n^i \qquad N = 1, 2, 3, 4\,. \tag{3.7}$$

Secondly, the exponent estimates $\Delta_n = n(R_n x_c^* - 1)$ and their extrapolants must simultaneously approach zero as $n \to \infty$. Some typical extrapolant values for the FCC lattice are shown in table 9. Choosing the p value which gives the smallest linear extrapolant of Δ_n, and 'flattest' extrapolant of R_n, we estimate the critical parameters:

$$\text{SC lattice:} \quad x_c = 0.19386(2) \qquad p = 0.33(5) \tag{3.8}$$

$$\text{BCC lattice:} \quad x_c = 0.14071(8) \qquad p = 0.32(4) \tag{3.9}$$

$$\text{FCC lattice:} \quad x_c = 0.09206(2) \qquad p = 0.32(4)\,. \tag{3.10}$$

These results are in good agreement with the RG prediction $p = \frac{1}{3}$.

3.3. *Critical amplitudes*

The renormalization group analysis also provides universal predictions for ratios of the amplitudes of the singular terms at the critical point (Brezin *et al* 1976). To be specific, suppose a quantity $f(t)$ has singular behaviour

$$f(t) \overset{t \to 0}{\sim} F^{\pm}|t|^{-q}|\ln|t||^p \tag{3.11}$$

where $F^+(F^-)$ is the critical amplitude at high (low) temperature, or strong (weak) coupling, respectively. Then the ratios F^+/F^- are predicted to take their mean-field values:

$$\text{specific heat:} \quad A^+/A^- = \tfrac{1}{4} \tag{3.12}$$

$$\text{susceptibility:} \quad C^+/C^- = 2 \tag{3.13}$$

$$\text{energy gap:} \quad f^+/f^- = 1/\sqrt{2}\,. \tag{3.14}$$

Table 9. Analysis of the transformed high-temperature susceptibility series for the FCC lattice, assuming $x_c^* = 0.09207$ in the Euler transformation.

p^*	n	R_n	Linear extrapolants $1/R_\infty$	Quadratic extrapolants $1/R_\infty$	$N = 3$ extrapolants $1/R_\infty + c_1/n$	$N = 4$ extrapolants $1/R_\infty + c_1/n$	Exponent Δ_n	Linear extrapolants of Δ_n
0.3	6	0.092 497 9	0.091 475 8	0.091 946 1	$0.092\,096 + 0.156/n$	$0.092\,134 + 0.236/n$	−0.027 758 3	0.004 718 64
0.3	7	0.092 372 8	0.091 628 8	0.092 013 4	$0.092\,103\,3 + 0.169/n$	$0.092\,108\,7 + 0.183/n$	−0.022 943	0.005 948 6
0.3	8	0.092 292 2	0.091 732	0.092 043	$0.092\,092\,3 + 0.145/n$	$0.092\,081\,4 + 0.112/n$	−0.019 258 2	0.006 535 37
0.3	9	0.092 237 6	0.091 803 6	0.092 055 3	$0.092\,079\,9 + 0.115/n$	$0.092\,064\,4 + 0.0599/n$	−0.016 356 8	0.006 854 55
0.3	10	0.092 199 2	0.091 854 8	0.092 059 9	$0.092\,070\,6 + 0.0882/n$	$0.092\,056\,5 + 0.0317/n$	−0.014 013 7	0.007 074 35
0.3	11	0.092 171 2	0.091 892 2	0.092 061 1	$0.092\,064\,4 + 0.0686/n$	$0.092\,053\,7 + 0.0204/n$	−0.012 079 1	0.007 267 31
0.3	12	0.092 150 3	0.091 920 3	0.092 061	$0.092\,060\,7 + 0.0553/n$	$0.092\,053\,2 + 0.0182/n$	−0.010 450 6	0.007 462 74
0.317	6	0.092 583 7	0.091 456 9	0.091 934 2	$0.092\,089\,2 + 0.101/n$	$0.092\,129 + 0.185/n$	−0.033 288 4	0.000 231 919
0.317	7	0.092 443 7	0.091 612 7	0.092 004 5	$0.092\,098\,4 + 0.117/n$	$0.092\,105\,2 + 0.135/n$	−0.028 296 3	0.001 655 97
0.317	8	0.092 352 4	0.091 718 1	0.092 036	$0.092\,088\,6 + 0.0961/n$	$0.092\,078\,8 + 0.066/n$	−0.024 459 9	0.002 394 83
0.317	9	0.092 289 7	0.091 791 6	0.092 049 6	$0.092\,076\,9 + 0.0672/n$	$0.092\,062\,3 + 0.0156/n$	−0.021 426 9	0.002 837 46
0.317	10	0.092 245	0.091 844 2	0.092 055 1	$0.092\,068 + 0.042/n$	$0.092\,054\,7 - 0.0114/n$	−0.018 968 2	0.003 160 19
0.317	11	0.092 211 9	0.091 882 8	0.092 057 1	$0.092\,062\,2 + 0.0237/n$	$0.092\,052\,1 - 0.0216/n$	−0.016 931	0.003 440 84
0.317	12	0.092 186 9	0.091 911 9	0.092 057 5	$0.092\,058\,8 + 0.0114/n$	$0.092\,051\,9 - 0.0229/n$	−0.015 210 7	0.003 712 24
0.333	6	0.092 669 7	0.091 438 2	0.091 922 1	$0.092\,082\,2 + 0.045/n$	$0.092\,124 + 0.134/n$	−0.038 826 6	−0.004 276 76
0.333	7	0.092 514 9	0.091 596 7	0.091 995 4	$0.092\,093\,4 + 0.0648/n$	$0.092\,101\,7 + 0.0865/n$	−0.033 659 4	−0.002 655 99
0.333	8	0.092 412 8	0.091 704 4	0.092 028 9	$0.092\,084\,7 + 0.0464/n$	$0.092\,076\,1 + 0.02/n$	−0.029 672 4	−0.001 763 02
0.333	9	0.092 342	0.091 779 6	0.092 043 9	$0.092\,073\,8 + 0.0194/n$	$0.092\,060\,2 - 0.0289/n$	−0.026 508 2	−0.001 195 37
0.333	10	0.092 290 9	0.091 833 6	0.092 050 3	$0.092\,065\,5 - 0.004\,26/n$	$0.092\,052\,9 - 0.0546/n$	−0.023 934 3	−0.000 768 415
0.333	11	0.092 252 8	0.091 873 4	0.092 053	$0.092\,060\,1 - 0.0214/n$	$0.092\,050\,6 - 0.0638/n$	−0.021 794 7	−0.000 399 037
0.333	12	0.092 223 6	0.091 903 5	0.092 054	$0.092\,056\,9 - 0.0327/n$	$0.092\,050\,5 - 0.0642/n$	−0.019 982 7	−0.000 050 788 2

Table 9. Continued.

p^*	n	R_n	Linear extrapolants $1/R_\infty$	Quadratic extrapolants $1/R_\infty$	$N=3$ extrapolants $1/R_\infty + c_1/n$	$N=4$ extrapolants $1/R_\infty + c_1/n$	Exponent Δ_n	Linear extrapolants of Δ_n
0.35	6	0.092 756	0.091 4197	0.091 9099	$0.092\,0751 - 0.0109/n$	$0.092\,1189 + 0.0821/n$	−0.044 3729	−0.008 807 29
0.35	7	0.092 5863	0.091 5809	0.091 9863	$0.092\,0883 + 0.0124/n$	$0.092\,0982 + 0.038/n$	−0.039 0321	−0.006 987 22
0.35	8	0.092 4734	0.091 6907	0.092 0217	$0.092\,0809 - 0.00341/n$	$0.092\,0734 - 0.0263/n$	−0.034 8953	−0.005 938 15
0.35	9	0.092 3944	0.091 7677	0.092 0381	$0.092\,0707 - 0.0286/n$	$0.092\,058 - 0.0735/n$	−0.031 6007	−0.005 243 89
0.35	10	0.092 337	0.091 8231	0.092 0455	$0.092\,0629 - 0.0507/n$	$0.092\,0511 - 0.0979/n$	−0.028 9118	−0.004 711 45
0.35	11	0.092 2938	0.091 8641	0.092 0489	$0.092\,0579 - 0.0667/n$	$0.092\,0491 - 0.106/n$	−0.026 67	−0.004 2523
0.35	12	0.092 2604	0.091 8951	0.092 0504	$0.092\,055 - 0.0769/n$	$0.092\,0492 - 0.106/n$	−0.024 7664	−0.003 826 33
0.375	6	0.092 886	0.091 3925	0.091 8913	$0.092\,0643 - 0.0955/n$	$0.092\,1112 + 0.00402/n$	−0.052 7066	−0.015 6438
0.375	7	0.092 6938	0.091 5575	0.091 9723	$0.092\,0806 - 0.0667/n$	$0.092\,0928 - 0.035/n$	−0.047 1086	−0.013 5201
0.375	8	0.092 5646	0.091 6704	0.092 0108	$0.092\,075 - 0.0786/n$	$0.092\,0693 - 0.0959/n$	−0.042 7491	−0.012 2332
0.375	9	0.092 4734	0.091 7499	0.092 0292	$0.092\,066 - 0.101/n$	$0.092\,0547 - 0.141/n$	−0.039 2599	−0.011 3461
0.375	10	0.092 4064	0.091 8074	0.092 0381	$0.092\,0589 - 0.121/n$	$0.092\,0484 - 0.163/n$	−0.036 3992	−0.010 653
0.375	11	0.092 3555	0.091 85	0.092 0426	$0.092\,0545 - 0.135/n$	$0.092\,0468 - 0.17/n$	−0.034 0045	−0.010 0573
0.375	12	0.092 3159	0.091 8825	0.092 045	$0.092\,0521 - 0.144/n$	$0.092\,0472 - 0.168/n$	−0.031 9635	−0.009 513 09

Since we have both strong-coupling and weak-coupling series to hand, we can attempt to check these predictions.

Biased estimates of the amplitude ratios can be obtained by the following technique. Assuming that the singular behaviour predicted by RG theory is correct, and an accurate estimate of the critical point is available, one can extrapolate the strong-coupling and weak-coupling series using integrated differential approximants (Guttmann 1989) to estimate the function f at points $\pm t$, equidistant from the critical point on either side. Then

$$\frac{F^+}{F^-} = \lim_{t\to 0} \frac{f(+t)}{f(-t)} \tag{3.15}$$

where $t = 1 - x/x_c$ for the strong-coupling side, or $t = 1 - \lambda_c/\lambda$ for the weak-coupling side. Because each quantity varies rapidly near the critical point, it is useful to 'smooth' each of these functions before making the extrapolations, by calculating approximants to the series for $|t|^q |\ln|t||^{-p} f(t)$ rather than $f(t)$ itself.

Specific heat. The behaviour of the specific heat itself, reconstructed from the extrapolation procedure, is shown in figure 1. The ratio $C(+t)/C(-t)$ is graphed as a function of t in figure 2. Near the critical point ($t = 0$), we estimate that

$$C = \begin{cases} 0.112(6)\left[-\ln\left(1 - x^2/x_c^2\right)/\left(x^2/x_c^2\right)\right]^{1/3} & \text{(SC lattice)} \\ 0.101(6)\left[-\ln\left(1 - x^2/x_c^2\right)/\left(x^2/x_c^2\right)\right]^{1/3} & \text{(BCC lattice)} \\ 0.092(5)\left[-\ln\left(1 - x^2/x_c^2\right)/\left(x^2/x_c^2\right)\right]^{1/3} & \text{(FCC lattice)} \end{cases} \tag{3.16}$$

from the strong-coupling side, or

$$C' = \begin{cases} 0.8866(6)\left[-\ln\left(1 - \lambda^2/\lambda_c^2\right)/\left(\lambda^2/\lambda_c^2\right)\right]^{1/3} & \text{(SC lattice)} \\ 0.849(10)\left[-\ln\left(1 - \lambda^2/\lambda_c^2\right)/\left(\lambda^2/\lambda_c^2\right)\right]^{1/3} & \text{(BCC lattice)} \\ 0.84(1)\left[-\ln\left(1 - \lambda^2/\lambda_c^2\right)/\left(\lambda^2/\lambda_c^2\right)\right]^{1/3} & \text{(FCC lattice)} \end{cases} \tag{3.17}$$

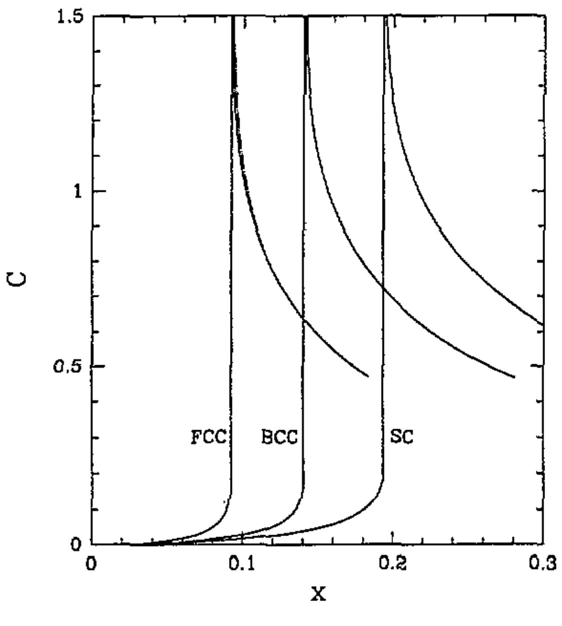

Figure 1. The specific heat as a function of coupling x for each of the three lattices.

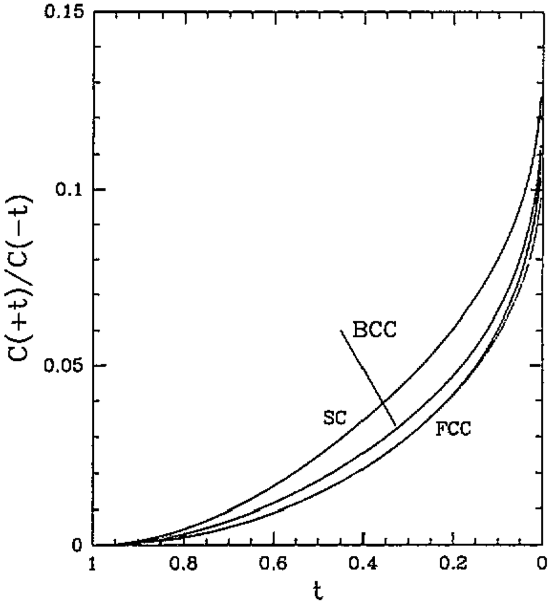

Figure 2. The ratio of the specific heats at reduced couplings $\pm t$, as a function of t, for each lattice.

from the weak-coupling side. Thus the critical amplitude ratio is found to be

$$\frac{A^+}{A^-} = \lim_{t\to 0}\frac{C(+t)}{C'(-t)} = \begin{cases} 0.13(1) & (\text{SC lattice}) \\ 0.12(1) & (\text{BCC lattice}) \\ 0.11(2) & (\text{FCC lattice}) \end{cases} \tag{3.18}$$

these values are a factor of 2 lower than the RG prediction. We remark that the ratio in figure 2 is curving steeply upward as $t \to 0$, and the error bounds in (3.18) may well be underestimated.

It is worth noting at this point that Ahlers *et al* (1975) have performed a least-squares fit to experimental data for the specific heat of a system belonging to the same universality class as the present model, and found excellent agreement with the expected amplitude ratio $A^+/A^- = \frac{1}{4}$. They were able to obtain accurate data at extremely small values of t, $|t| \leqslant 0.001$, whereas our present series extrapolations become highly unreliable at such small t values.

Magnetization. Near the critical point on the weak-coupling side, the magnetization is found to be

$$M = \begin{cases} 0.43(1)\left(1-\lambda^2/\lambda_c^2\right)^{1/2}\left[-\ln\left(1-\lambda^2/\lambda_c^2\right)/\left(\lambda^2/\lambda_c^2\right)\right]^{1/3} & (\text{SC lattice}) \\ 0.42(1)\left(1-\lambda^2/\lambda_c^2\right)^{1/2}\left[-\ln\left(1-\lambda^2/\lambda_c^2\right)/\left(\lambda^2/\lambda_c^2\right)\right]^{1/3} & (\text{BCC lattice}) \\ 0.42(1)\left(1-\lambda^2/\lambda_c^2\right)^{1/2}\left[-\ln\left(1-\lambda^2/\lambda_c^2\right)/\left(\lambda^2/\lambda_c^2\right)\right]^{1/3} & (\text{FCC lattice}). \end{cases} \tag{3.19}$$

The critical amplitude appears to be universal for all three lattices. In fact, if the magnetization estimates are plotted against the 'reduced' coupling variable λ/λ_c, as in figure 3, they lie very nearly on a universal curve at all couplings, obeying an approximate 'law of corresponding states'.

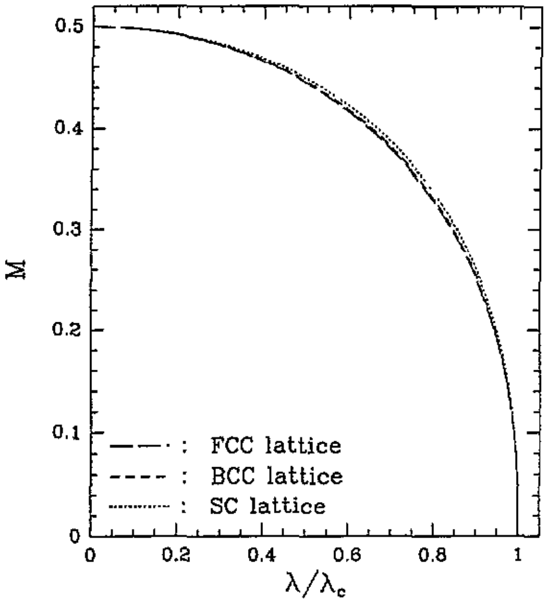

Figure 3. The magnetization M as a function of reduced coupling λ/λ_c for each of the three lattices.

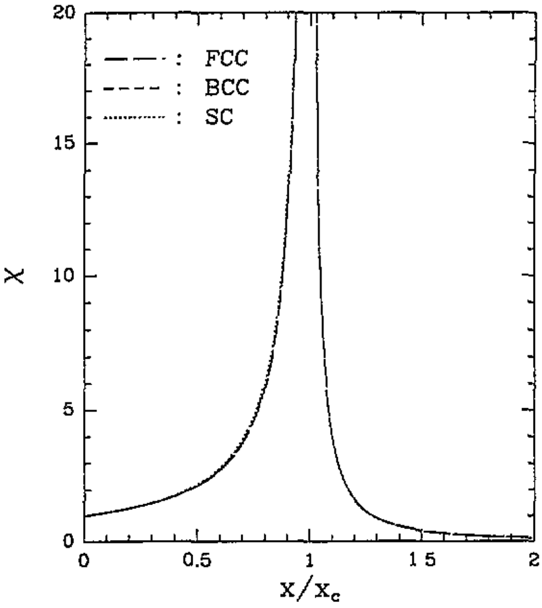

Figure 4. The susceptibility χ as a function of reduced coupling x/x_c for all three lattices.

Susceptibility. The susceptibility χ (though *not* χ') similarly appears to obey a 'law of corresponding states', as seen in figure 4. Near the critical point, it is found to be

$$\chi = \begin{cases} 0.92(4)(1 - x/x_c)^{-1}[-\ln(1 - x/x_c)/(x/x_c)]^{1/3} & \text{(SC lattice)} \\ 0.86(5)(1 - x/x_c)^{-1}[-\ln(1 - x/x_c)/(x/x_c)]^{1/3} & \text{(BCC lattice)} \\ 0.86(6)(1 - x/x_c)^{-1}[-\ln(1 - x/x_c)/(x/x_c)]^{1/3} & \text{(FCC lattice)} \end{cases} \tag{3.20}$$

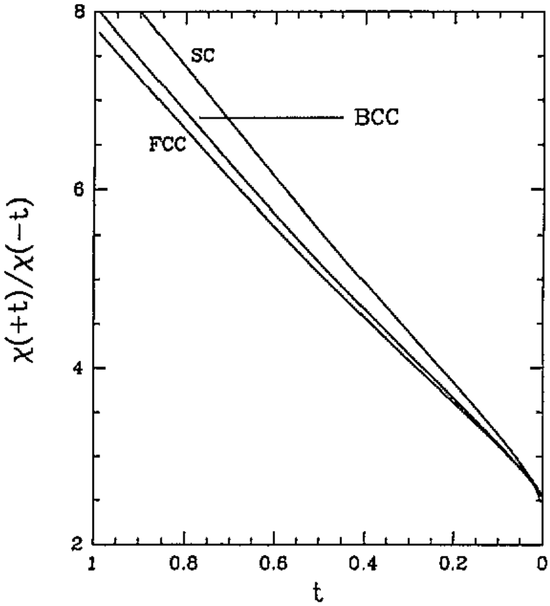

Figure 5. The ratio of the susceptibilities at $\pm t$ as a function of t for each lattice.

from the strong-coupling side, and

$$\chi' = \begin{cases} 0.15(3)\left(1-\lambda^2/\lambda_c^2\right)^{-1}\left[-\ln\left(1-\lambda^2/\lambda_c^2\right)/\left(\lambda^2/\lambda_c^2\right)\right]^{1/3} & (\text{SC lattice}) \\ 0.104(8)\left(1-\lambda^2/\lambda_c^2\right)^{-1}\left[-\ln\left(1-\lambda^2/\lambda_c^2\right)/\left(\lambda^2/\lambda_c^2\right)\right]^{1/3} & (\text{BCC lattice}) \\ 0.066(6)\left(1-\lambda^2/\lambda_c^2\right)^{-1}\left[-\ln\left(1-\lambda^2/\lambda_c^2\right)/\left(\lambda^2/\lambda_c^2\right)\right]^{1/3} & (\text{FCC lattice}) \end{cases} \tag{3.21}$$

from the weak-coupling side, so that the ratio

$$\frac{C^+}{C^-} = \lim_{t\to 0}\frac{\chi(+t)}{4\lambda_c\chi'(-t)} = \begin{cases} 2.4(5) & (\text{SC lattice}) \\ 2.3(3) & (\text{BCC lattice}) \\ 2.4(4) & (\text{FCC lattice}). \end{cases} \tag{3.22}$$

The ratio is curving rapidly downwards as $t \to 0$ (see figure 5), so that these results appear reasonably consistent with the RG prediction $C^+/C^- = 2$, at a 20% level of accuracy. The amplitude for χ itself appears to be universal, in fact, for these three lattices.

Energy gap. The energy gap also behaves in a nearly universal fashion, as shown in figure 6. Near the critical point, it behaves as

$$m = \begin{cases} 2.05(8)(1-x/x_c)^{1/2}[-\ln(1-x/x_c)/(x/x_c)]^{-1/6} & (\text{SC lattice}) \\ 2.09(7)(1-x/x_c)^{1/2}[-\ln(1-x/x_c)/(x/x_c)]^{-1/6} & (\text{BCC lattice}) \\ 2.11(5)(1-x/x_c)^{1/2}[-\ln(1-x/x_c)/(x/x_c)]^{-1/6} & (\text{FCC lattice}) \end{cases} \tag{3.23}$$

from the strong-coupling side, and

$$m' = \begin{cases} 2.80(2)\left(1-\lambda^2/\lambda_c^2\right)^{1/2}\left[-\ln\left(1-\lambda^2/\lambda_c^2\right)/\left(\lambda^2/\lambda_c^2\right)\right]^{-1/6} & (\text{SC lattice}) \\ 3.95(3)\left(1-\lambda^2/\lambda_c^2\right)^{1/2}\left[-\ln\left(1-\lambda^2/\lambda_c^2\right)/\left(\lambda^2/\lambda_c^2\right)\right]^{-1/6} & (\text{BCC lattice}) \\ 6.09(3)\left(1-\lambda^2/\lambda_c^2\right)^{1/2}\left[-\ln\left(1-\lambda^2/\lambda_c^2\right)/\left(\lambda^2/\lambda_c^2\right)\right]^{-1/6} & (\text{FCC lattice}) \end{cases} \tag{3.24}$$

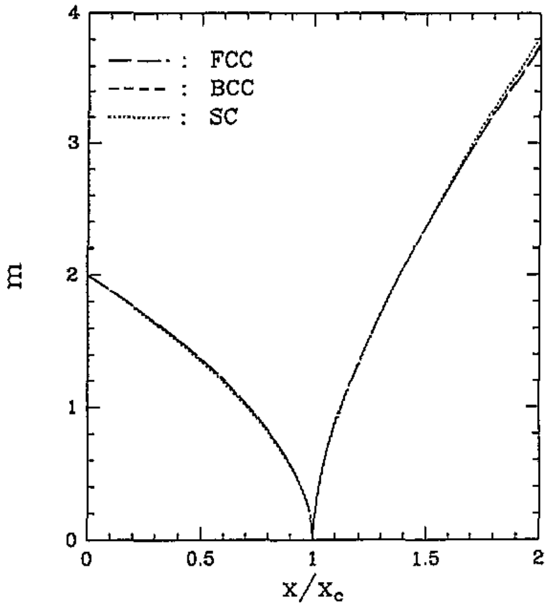

Figure 6. The energy gap m as a function of reduced coupling x/x_c for all three lattices.

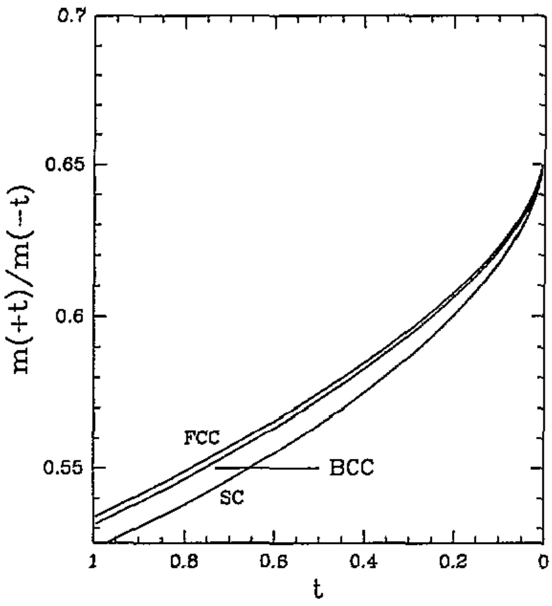

Figure 7. The ratio of energy gaps at $\pm t$, as a function of t for each lattice.

from the weak-coupling side. The amplitude ratio is

$$\frac{f^+}{f^-} = \lim_{t\to 0} \frac{m(+t)}{m'(-t)/\lambda_c} = \begin{cases} 0.67(3) & (\text{SC lattice}) \\ 0.67(3) & (\text{BCC lattice}) \\ 0.67(2) & (\text{FCC lattice})\,. \end{cases} \tag{3.25}$$

Since these ratios are curving upwards as $t \to 0$ (figure 7), these estimates again seem quite compatible with the RG prediction $f^+/f^- = 1/\sqrt{2}$, at about a 5% level of accuracy. The energy gap amplitudes themselves appear to be universal for these three lattices.

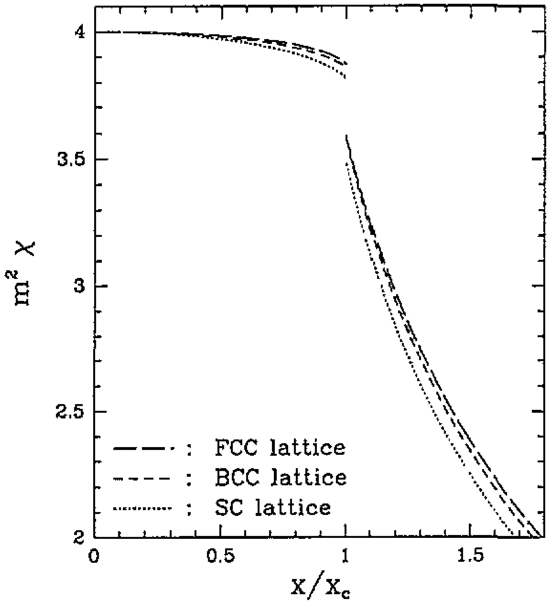

Figure 8. The product $m^2\chi$ as a function of reduced coupling x/x_c for all three lattices.

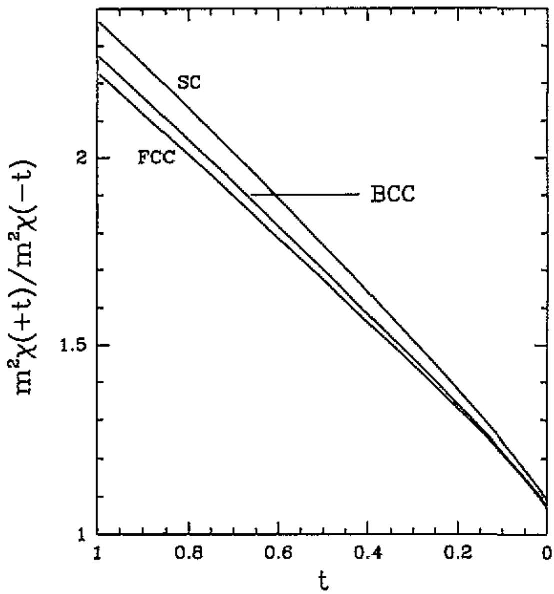

Figure 9. The ratio of $m^2\chi$ at $\pm t$, as a function of t for each lattice.

A final test can be obtained by extrapolating the series for $m^2\chi$, which is predicted to approach a constant value at the critical point. Figure 8 shows the results for this quantity. Near the critical point,

$$m^2\chi = \begin{cases} 3.80(4) & (\text{SC lattice}) \\ 3.85(6) & (\text{BCC lattice}) \\ 3.87(4) & (\text{FCC lattice}) \end{cases} \tag{3.26}$$

from the strong-coupling side, and

$$m'^2\chi' = \begin{cases} 1.13(4) & (\text{SC lattice}) \\ 1.63(10) & (\text{BCC lattice}) \\ 2.44(4) & (\text{FCC lattice}) \end{cases} \tag{3.27}$$

from the weak-coupling side. The amplitude ratio is shown in figure 9, and at the critical point it is found to be

$$\lim_{t\to 0} \frac{m^2\chi(+t)}{4m'^2\chi'(-t)/\lambda_c} = \begin{cases} 1.08(5) & (\text{SC lattice}) \\ 1.05(8) & (\text{BCC lattice}) \\ 1.08(5) & (\text{FCC lattice}). \end{cases} \tag{3.28}$$

According to (3.12)–(3.14) this ratio should be exactly 1. The result (3.28) is in fairly good agreement with the prediction, at about a 5–10% level of accuracy. The results (3.26) are also in good agreement with the combined results (3.23) and (3.20), which provides evidence that the extrapolation procedure is consistent.

4. Conclusions

The results of the series analysis have mostly been consistent with the predictions of renormalization group theory. Firstly, the power-law exponents at the critical point were found to be consistent with the mean field values to within 5% or less. Then, assuming these exponents do take their mean field values, the exponents of the confluent logarithmic terms were found to be consistent with the predicted values at a 10–20% level of accuracy. And finally, assuming both power laws and logarithms have the predicted exponents, the ratios of the critical amplitudes above and below the critical point were found to approach their expected universal values for the susceptibility and energy gap, within accuracies ranging from 5–20%.

An exception is the critical amplitude ratio for the specific heat, which disagrees with the predicted value by a factor of two. The ratio is curving sharply upwards near the critical point, however, and the singularity in the specific heat is weak, so we do not place too much weight on this discrepancy.

The results also show a remarkable degree of universality between the three different lattices considered. When graphed against the 'reduced' coupling or 'temperature' variable, the results for the magnetization, susceptibility and energy gap are virtually indistinguishable for all three lattices, not only near the critical point but at all couplings. Even the specific heats are not very different. A 'law of corresponding states' seems to be obeyed very closely in this system.

Acknowledgment

This work forms part of a research project supported by a grant from the Australian Research Council.

References

Ahlers G, Kornblit A and Guggenheim H J 1975 *Phys. Rev. Lett.* **34** 34 1227
Baker G A Jr 1977 *Phys. Rev* B **15** 1552
Birgeneau R J 1972 *AIP Conf. Proc. No. 10 Magnetism and Magnetic Materials* ed C D Graham and J J Rhyne p 1664

Brezin E, Le Guillou J C and Zinn-Justin J 1973 *Phys. Rev.* D **8** 2418
——1976 *Phase Transitions and Critical Phenomena* vol 6 ed C Domb and M S Green (New York: Academic)
Elliott R J and Wood C 1971 *J. Phys., C: Solid State Phys.* **4** 2359
Fisher M E and Gaunt D S 1964 *Phys. Rev.* A **133** 224
Fradkin E and Susskind L 1978 *Phys. Rev.* D **17** 2637
Gaunt D S, Sykes M F and McKenzie S 1979 *J. Phys. A: Math. Gen.* **12** 871
Green M B, Sneddon L and Stinchcombe R B 1979 *J. Phys. A: Math. Gen.* **12** L189
Guttmann A J 1978 *J. Phys. A: Math. Gen.* **11** L103
——1989 *Phase Transitions and Critical Phenomena* vol 13 ed C Domb and J Lebowitz (New York: Academic)
He H X, Hamer C J and Oitmaa J 1990 *J. Phys. A: Math. Gen.* **24** 2863
Jansen K, Montvay I, Münster G, Trappenberg T and Wolff U 1989 *Nucl. Phys.* B **322** 698
Larkin A I and Khmel'Nitskii D E 1969 *Zh. Eksp. Teor. Fiz.* **56** 2087; *Sov. Phys.–JETP* **29** 1123
Moore M A 1970 *Phys. Rev.* B **1** 2238
Nickel B G 1980 unpublished
Oitmaa J and Coombs G J 1981 *J. Phys. C: Solid State Phys.* **14** 143
Oitmaa J and Plischke 1976 *J. Phys. C: Solid State Phys.* **9** 2093
Oitmaa J, Hamer C J and Zheng W H 1991 *J. Phys. A: Math. Gen.* **23** 1775
Pfeuty P 1976 *J. Phys. C: Solid State Phys.* **9** 3993
Pfeuty P and Elliott R J 1971 *J. Phys. C: Solid State Phys.* **4** 2370
Stinchcombe R B 1972 *J. Phys. C: Solid State Phys.* **6** 2459
Suzuki M 1976 *Prog. Theor. Phys.* **56** 1454
Vohwinkel C and Weisz P 1992 *Nucl. Phys.* B **374** 647
Wegner F J and Riedel E K 1973 *Phys. Rev.* B **7** 248
Yanase A 1977 *J. Phys. Soc. Japan* **42** 1816
Yanase A, Takeshige Y and Suzuki M 1976 *J. Phys. Soc. Japan* **41** 1108